Journal of Industrial and Systems Engineering
Vol. 17, No. 3, pp. 93-121
Summer (July) 2025

JISE

Integrated Location-Allocation Modeling and Optimization in Relief Supply Chain Networks: A Hybrid Machine Learning and Fuzzy Analysis Approach

Omid Veisi[1*]

1Faculty of Engineering and Aviation, Imam Ali University, Tehran, Iran

Abstract

Efficient crisis management following natural disasters, particularly earthquakes, necessitates optimal resource allocation, appropriate facility location, and precise transportation planning. In this study, a multi-stage mathematical model is proposed for the design and optimization of a relief supply chain network comprising distribution centers, temporary shelters, temporary care centers, and hospitals. Aiming to minimize total operational costs and reduce shortages of relief items, the model simultaneously optimizes location, allocation, and transportation decisions. To achieve dynamic and realistic demand forecasting for relief items in temporary shelters, time-series-based machine learning algorithms are utilized. Furthermore, by employing fuzzy logic, uncertainty in the capacity of vehicles and medical centers is modeled and incorporated into the decision-making process. The proposed model is formulated as a Mixed-Integer Linear Programming (MILP) problem and utilizes the weighted sum method to integrate multiple objectives. Results indicate that integrating machine learning-based demand forecasting with fuzzy uncertainty management significantly enhances the efficiency of the relief network, reduces response time and total costs, and improves the service level provided to the victims. This approach presents a robust, data-driven framework for decision-making in critical conditions, which can serve as a decision support tool for relief organizations.

Keywords: Crisis Management, Multi-stage Optimization, Machine Learning, Fuzzy Logic, Demand Forecasting, Relief Supply Chain.

1- Introduction

Crisis management, particularly following natural disasters, plays a pivotal role in minimizing casualties and mitigating disruptions to critical infrastructure. Incidents such as earthquakes

* Corresponding Author

and floods cause sudden devastation, creating an immediate need for shelter, medical care, and the distribution of relief items (Geng et al., 2024). The efficiency of the response during the initial hours relies heavily on the optimal allocation of resources, accessibility of relief centers, and the coordination of transportation (Saeidian et al., 2018).

One of the most significant challenges in such conditions is the simultaneous management of the flow of people and goods under strict time constraints and variable capacities (Ahmad et al., 2025). Following an earthquake, determining appropriate locations for temporary care centers, temporary shelters, and hospitals is essential to ensure the evacuation of the injured and the distribution of vital items with minimal delay (Setiawan et al., 2019; Emami et al., 2024). A multi-stage relief supply chain network can facilitate this process through the optimization of location and allocation decisions (Jha et al., 2017; Nozari et al., 2023).

Accurate demand forecasting for relief items constitutes a key dimension of this network. Crisis situations are typically characterized by fluctuation and uncertainty, rendering classical demand estimation methods limited in efficiency. By analyzing temporal and data-driven patterns, Machine Learning (ML) algorithms enable dynamic and realistic demand forecasting (Baygan et al., 2024; Ghasemi et al., 2022; aliahmadi et al., 2013). Furthermore, the presence of uncertainty in the capacities of hospitals, vehicles, and infrastructure necessitates approaches capable of incorporating this ambiguity into the model. Fuzzy logic serves as a suitable tool for modeling such uncertainties and has been widely employed in recent research.

Previous studies have each examined specific segments of the relief chain, such as shelter location, resource allocation, or route design; however, in most instances, these decisions have been made in isolation without considering the interdependencies between different stages. Moreover, many approaches have assumed fixed demand or demand estimated via simple methods, which can lead to low-accuracy decision-making in turbulent environments.

While recent robust and stochastic optimization models—such as the multi-scenario resource allocation by Ma and Chiang (2024) and the distributionally robust shelter planning by Tang and Osaragi (2024)—have significantly advanced decision-making under uncertainty, they often rely on static or broad stochastic bounds for demand. Our proposed hybrid approach outperforms these traditional baselines by integrating high-precision machine learning directly into the optimization framework. Specifically, our comparative analysis (detailed in Section 4) demonstrates that the incorporated Seasonal ARIMA (SARIMA) model achieves a Mean Absolute Percentage Error (MAPE) of 3.61%, reducing forecast error by approximately 84% compared to standard time-series baselines used in conventional planning (which exhibited MAPEs exceeding 23%). By feeding these highly accurate, dynamic demand signals into a fuzzy MILP framework, the proposed model minimizes the 'cost of uncertainty,' allowing for a verified 80% minimum service level without the excessive over-stocking typically required by standard robust models to mitigate high-variance demand.

Aiming to bridge this gap, this research presents an integrated model for designing a relief supply chain network in which facility location, assignment of affected areas, flow of people, distribution of multi-item relief goods, and fleet allocation are coordinated within a harmonized mathematical framework. To account for demand dynamics, a time-series-based machine learning model is utilized, and sensitive capacities are modeled using fuzzy numbers. The combination of machine learning and fuzzy logic with an integer linear programming model provides a robust, data-driven framework for decision-making in post-earthquake conditions.

2- Literature review

Effective coordination in post-disaster relief necessitates the simultaneous management of resource allocation, facility location, and evacuation planning. While numerous studies have addressed each of these domains individually, the integration of these three components within a single unified framework remains relatively scarce (Basu et al., 2018; Wang et al., 2020).

Resource Allocation

Efficient resource allocation constitutes a fundamental challenge in crisis situations, as the severity and pattern of damage are highly variable, and needs shift rapidly. Recent studies emphasize demand forecasting and proactive resource allocation. Deep learning-based models for needs prediction (Zhang et al., 2024; Movahed et al., 2024) and two-stage approaches for integrating pre- and post-disaster planning (Yang et al., 2022) are examples of such efforts. Furthermore, the utilization of real-time capabilities, such as satellite communications (Xie et al., 2024), and social equity indicators (Long et al., 2024) demonstrates that efficiency is not the sole criterion for decision-making. In emerging fields, the combination of blockchain and machine learning has been proposed to enhance transparency and improve resource allocation (Raj et al., 2024). Multi-scenario robust models have also gained importance for addressing severe crisis uncertainties (Ma & Chiang, 2024). Alongside physical resources, the management of volunteers is also of significant importance (Ghasemi et al., 2023). Overall, recent literature indicates that data-driven and robust approaches can significantly improve accuracy and equity in resource allocation.

Optimization of Shelter Location

The optimal location of shelter and care centers plays a vital role in reducing response time and improving population coverage. Many studies have focused on integrating criteria such as equity, capacity, accessibility, and geographical features (Mao & Ma, 2025). Some studies have combined multi-echelon location structures with inventory management (Veisi et al., 2019), while others have addressed specific characteristics of vital aid chains, such as perishable goods (Chobar et al., 2025). Fuzzy approaches have also been employed to model uncertainty and convert multiple objectives (Jabal-Ameli et al., 2011). Robust models have found widespread application in conditions characterized by demand fluctuations or severe capacity constraints (Tang & Osaragi, 2024; Iraj et al., 2024). Studies based on Geographic Information Systems (GIS) have also been utilized to identify suitable locations for flood or earthquake shelters in various countries (Rahmawaty & Hasan, 2023; Saeedi & Dejpasand, 2024). Finally, advanced multi-objective models have been developed for the optimal allocation of shelters under technical, traffic, or security constraints (Batur et al., 2025; Woo & Kang, 2025).

Evacuation Planning

The success of evacuation depends on population behavior, transportation network capacity, and individual decision-making. Agent-based models and human behavior simulations (Bakhshian & Martinez-Pastor, 2023) have expanded in recent years due to their ability to

accurately represent congestion and population response. Studies have also focused on designing optimal routes using bio-inspired algorithms (Du et al., 2024). Some research has examined the role of social networks and public trust in the decision to evacuate (Salazar et al., 2024; Tang et al., 2025). Attention to vulnerable groups, such as the elderly, has also gained significant importance (Yazdani & Haghani, 2023). Moreover, compound disasters, such as the concurrence of an earthquake and a pandemic, have added new dimensions to decision analysis (Bahmani et al., 2023).

Technological Innovations in Post-Disaster Relief Coordination

Technologies such as Radio Frequency Identification (RFID), Unmanned Aerial Vehicles (UAVs) or drones, blockchain, GIS, cloud computing, social media, and Artificial Intelligence (AI) play a pivotal role in enhancing the speed and accuracy of relief operations (Pal et al., 2024; Wagner et al., 2024). The integration of drones with blockchain for the secure and rapid distribution of resources in hard-to-reach areas, or the utilization of cloud platforms for real-time data management, represent examples of such applications (Yuichi Koido, 2023). Social media is also effective in mobilizing volunteers and exchanging information, yet it generates coordination challenges (Bier et al., 2025). Furthermore, AI has become a crucial tool for forecasting, allocation, and crisis scenario analysis.

Machine Learning in Resource Allocation

ML possesses a distinct capability in analyzing historical and dynamic data and has assumed a significant role in demand forecasting, resource allocation, and flow optimization. Reinforcement Learning (RL)-based models have reported superior performance for multi-period and uncertain decision-making contexts (Yu et al., 2021). In decentralized environments, the combination of RL and Game Theory has been developed for resource allocation (Smyrnakis & Galla, 2014). The integration of predictive and reinforcement learning in cloud resource management (Ahamed et al., 2023) or the application of deep networks in forecasting demand within the blood supply chain (Naderipour & Salandari Rabari, 2024) demonstrates that ML can better manage uncertainty and severe fluctuations. In the infrastructure domain, the use of RL to maintain the stability of crisis-stricken communication networks has also gained importance (Lu, 2024).

Research Gaps

A review of the literature reveals that:

- Many studies examine only specific segments of the relief network, and the integration among location, allocation, forecasting, and transportation is less frequently observed.
- Models based on fixed demand or lacking precise forecasting do not align with the dynamic conditions of a crisis.
- Uncertainty regarding operational capacities is less reflected in classical models.
- The integration of Machine Learning and Fuzzy logic within a unified mathematical model remains limited.

This research aims to bridge these gaps by presenting an integrated, data-driven model.

3- Methodology

Problem description

This study addresses the design of a multi-stage relief supply chain network following an earthquake, wherein decisions regarding facility opening, population allocation, and the transportation planning of people and relief items must be made simultaneously. The network comprises affected areas (demand origins), temporary care centers (for outpatients), temporary shelters (for evacuees), hospitals (for the critically injured), and distribution centers (for supplying relief items). The objective is the timely provision of shelter, care, and logistics for the displaced population, aiming to minimize total costs and reduce item shortages within the framework of capacity and coverage constraints.

To account for demand dynamics, the demand for multi-item relief goods in temporary shelters over the time horizon is predicted using time-series-based Machine Learning algorithms and fed into the optimization model as an exogenous input. Consequently, instead of assuming fixed demand, real consumption patterns and fluctuations across different centers are reflected in the decision-making process.

The model is formulated as a Mixed-Integer Linear Programming MILP problem, in which:

- Location decisions determine which temporary care and shelter centers are to be opened;
- Allocation decisions specify to which temporary care and shelter center each affected area is assigned, and to which hospital the critically injured patients are dispatched;
- Transportation decisions determine the flow of people (healthy, outpatients, critically injured) and relief items, as well as the number of vehicles utilized on each route per time period.

The objective function is a weighted combination of operational costs (facility establishment, fleet operation, and distance-based transportation) and penalties for relief item shortages; such that adjusting the weights allows for an analysis of the trade-off between economic savings and service level. Service level constraints also ensure that each active temporary shelter receives at least a specified fraction of its demand in each period.

Given the uncertain nature of the crisis environment, certain key parameters are modeled using fuzzy logic. Specifically, hospital admission capacities and vehicle passenger capacities are represented by triangular fuzzy numbers and converted into effective crisp values through confidence-level-based defuzzification. This approach reflects operational uncertainty in capacities while preserving the linear structure of the model.

In summary, the proposed model presents an integrated framework for:

- Location-allocation of temporary care and shelter centers,
- Allocation of patients and evacuees,
- Fleet planning and distribution of multi-item relief goods,

within a multi-stage network, utilizing machine learning-based demand forecasting and fuzzy uncertainty management. Figure 1 illustrates the general overview of the problem, and Tables 1 and 2 present the deterministic and fuzzy notations used in the model.

The assumptions of the problem are outlined as follows:

- Demand Forecasting via Machine Learning: The period-by-period demand for each relief item at every temporary shelter is predicted by a machine learning module based on historical data and incorporated into the model as exogenous parameters; demand uncertainty is managed through minimum service levels and shortage penalties.
- Unique Allocation of Affected Areas: Each affected area is assigned to exactly one temporary care center and one active temporary shelter; these assignments must fall within the permissible coverage radius of each facility.
- Multi-period Horizon and Immediate Delivery: Decision-making occurs over discrete time periods, and all relief item shipments initiated within a period are received within the same period. Inventory at distribution centers is carried over between periods, and no new external supply is considered during the planning horizon.
- Aggregated People Flow and Full Admission of Critically Injured: Evacuation is modeled as an aggregate flow, assuming that all critically injured patients must be transferred to and hospitalized in one of the hospitals during the planning horizon; whereas outpatients and healthy individuals are assigned to temporary care centers and temporary shelters, respectively.
- Possibilistic Capacities for Sensitive Parameters: Hospital admission capacities and vehicle passenger carrying capacities are modeled as triangular fuzzy numbers and converted into crisp equivalents using a fixed confidence level; other capacities (such as relief item transport) are considered deterministic.
- Transportation Based on Truck-Equivalent and Constant Speed: Relief item transport capacity is modeled as a continuous truck-equivalent value, incorporating limits on the number of available trucks per period and maximum driving hours. Travel time is calculated based on a constant average speed and static distances between nodes.
- Minimum Service Level and Linear Shortage Penalty: Each active temporary shelter must receive at least a specified fraction of its total demand in every period; shortages beyond this level are permissible but penalized linearly based on the item type. Unmet demand is not backlogged (transferred between periods), and substitution between items or centers is not permitted.
- Linear Distance-Based Costs: Transportation costs for people and items are proportional to distance and vehicle type, assumed constant throughout the horizon. Fixed costs for establishing and operating centers are also included in the objective function.

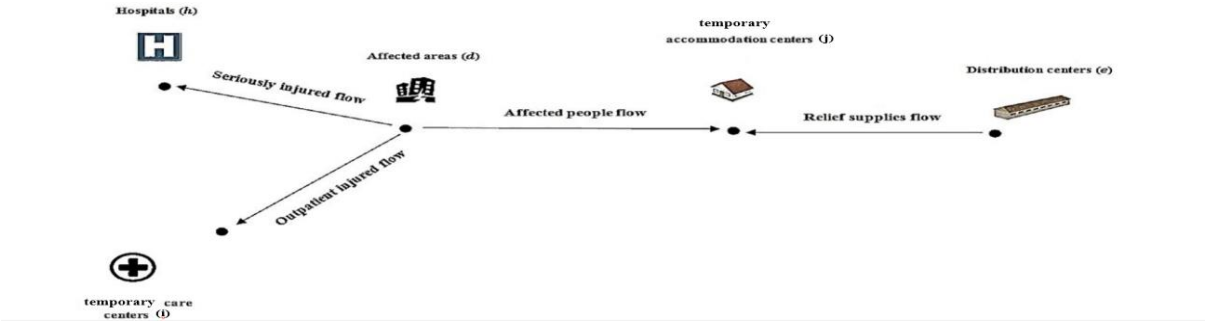

Figure 1. A graphic demonstration of the considered relief chain network

Table 1. Notations

Symbol	Description
Sets and Indices	
D	Set of affected areas
I	Set of temporary care centers
J	Set of temporary shelters
H	Set of hospitals
E	Set of distribution centers (DCs)
V	Set of vehicle types
C	Set of relief items (commodities)
T	Set of discrete time periods
Costs, Distances, and Coverage	
A_i	Establishment cost of temporary care center i
Ap_j	Establishment cost of temporary shelter j
App_v	Operation cost of vehicle v per unit distance
O_{di}	Distance between affected area d and temporary care center i
OP_{dj}	Distance between affected area d and temporary shelter j
OPP_{ej}	Distance between distribution center e and temporary shelter j
$OPPP_{dh}$	Distance between affected area d and hospital h
Q_i	Permissible coverage radius of temporary care center i
QP_j	Permissible coverage radius of temporary shelter j
Demand and Capacities	
B_d	Number of outpatients in affected area d
BP_d	Number of evacuees (people requiring shelter) in affected area d
BPP_d	Number of critically injured patients in affected area d
NP_{jc}	Handling/reception capacity of temporary shelter j for item c per period
NP_{ec}	Initial inventory of item c at distribution center e

DE_{cj}	Total demand for item c at temporary shelter j over the planning horizon
DE_{cjt}	Demand for item c at temporary shelter j during period t (Predicted/Exogenous)
Fleet and Transport Capacities	
M_v	Passenger carrying capacity of vehicle v (for outpatients/critically injured)
MPP_v	Cargo carrying capacity of vehicle v (truck-equivalent) per period
F_v	Number of available truck-equivalents of type v in each period
$HrsMax$	Maximum driving hours allowed for each vehicle in a period
$Speed$	Average travel speed
Service and Objective Weights	
SL	Minimum service level required for active temporary shelters in each period
W_1, W_2	Weights of objective functions (cost vs. shortage)
Ψ_c	Priority weight (penalty coefficient) for shortage of item c
$BigM$	Large constant for activating people flows
Big-M Constants and Model Strengthening	
M_{max}^I	Big-M parameter for coverage constraint of O_{di}
M_{max}^J	Big-M parameter for coverage constraint of OP_{dj}
M_c^E	Big-M parameter for activating route from j to e
Time Auxiliary Parameters	
St_{ect}	Inflow/supply injection of item c at distribution center e at time t
$TotDEt_{jt}$	Total demand of period t at temporary shelter j (aggregated over items)
Decision Variables	
X_i	1 if temporary care center i is opened, 0 otherwise
XP_j	1 if temporary shelter j is opened, 0 otherwise
Z_{di}	1 if affected area d is assigned to care center i, 0 otherwise
ZP_{dj}	1 if affected area d is assigned to shelter j, 0 otherwise
Y_{je}	1 if route from DC e to shelter j is active, 0 otherwise
U_{vdi}	Number of vehicles of type v on route d to i (transporting outpatients)
UP_{vdj}	Number of vehicles of type v on route d to i (transporting evacuees)
UPP_{vdh}	Number of vehicles of type v on route d to h (transporting critically injured)
L_{di}	Flow of outpatients from d to i
LP_{dj}	Flow of evacuees from d to j

LPP_{dh}	Flow of critically injured from d to h
Gt_{ejct}	Amount of item c transported from e to j in period t
Wt_{cjt}	Shortage of item c at shelter j in period t
Inv_{ect}	Inventory of item c at DC e at the end of period t
$UPPc_{vejt}$	Continuous truck-equivalent of type v on route e to j in period t

Table 2. Fuzzy symbols

Fuzzy Symbol	Description	Crisp Equivalent
$(MPPP_v, MPM_v, MPO_v)$	Triangular fuzzy passenger capacity of vehicle v for transporting evacuees	$\widehat{M}_v(\beta) = (1-\beta) \cdot \frac{MPM_v + MPO_v}{2} + \beta \cdot \frac{MPM_v + MPPP_v}{2}$
$(NPPP_h, NPPM_h, NPPO_h)$	Triangular fuzzy admission capacity of hospital h	$\widehat{H}_h(\beta_0) = (1-\beta_0) \cdot \frac{NPPM_h + NPPO_h}{2} + \beta_0 \cdot \frac{NPPM_h + NPPP_h}{2}.$
β, β_0	Confidence/caution parameter in defuzzification (ranging from 0 [optimistic] to 1 [pessimistic])	-

$$\text{minOBJ} = w_1 Z_1 + w_2 Z_2 \quad (1)$$

$$Z_1 = \sum_{i\in I} A_i X_i + \sum_{j\in J} AP_j XP_j + \sum_{v\in V} \text{APP}_v \left[\sum_{d\in D}\sum_{j\in J} OP_{dj} UP_{vdj} + \sum_{d\in D}\sum_{i\in I} O_{di} U_{vdi} + \sum_{e\in E}\sum_{j\in J}\sum_{t\in T} OPP_{ej} UPI \right. \left. \sum_{d\in D}\sum_{h\in H} OPPP_{dh} UPP_{vdh} \right] \quad (2)$$

$$Z_2 = \sum_{j\in J}\sum_{c\in C}\sum_{t\in T} \Psi_c Wt_{cjt} \quad (3)$$

$$\sum_i Z_{di} = 1 \qquad (\forall d) \quad (4)$$

$$\sum_j ZP_{dj} = 1 \qquad (\forall d) \quad (5)$$

$$O_{di} \le Q_i + M^I_{\max}(1 - Z_{di}) \qquad (\forall d, i) \quad (6)$$

$$OP_{dj} \le QP_j + M^J_{\max}\left(1 - ZP_{dj}\right) \qquad (\forall d, j) \quad (7)$$

$$Z_{di} \le X_i \ (\forall d, i), ZP_{dj} \le XP_j \qquad (\forall d, j) \quad (8\text{-}9)$$

$$L_{di} \leq \text{BigM} Z_{di}\ (\forall d,i), LP_{dj} \leq \text{BigM} ZP_{dj} \qquad (\forall d,j) \qquad (10\text{-}11)$$

$$\sum_{h} LPP_{dh} = BPP_{d} \qquad (\forall d) \qquad (12)$$

$$\sum_{i} L_{di} = B_{d} \qquad (\forall d) \qquad (13)$$

$$\sum_{j} LP_{dj} = BP_{d} \qquad (\forall d) \qquad (14)$$

$$L_{di} \leq \sum_{v} M_{v} U_{vdi} \qquad (\forall d,i) \qquad (15)$$

$$LP_{dj} \leq \sum_{v} \widehat{M}_{v}(\beta) UP_{vdj} \qquad (\forall d,j) \qquad (16)$$

$$LPP_{dh} \leq \sum_{v} M_{v} UPP_{vdh} \qquad (\forall d,h) \qquad (17)$$

$$\sum_{d} LPP_{dh} \leq \widehat{H}_{h}(\beta) \qquad (\forall h) \qquad (18)$$

$$\sum_{e} Gt_{ejct} + Wt_{cjt} \geq \text{DE}_{cjt} \qquad (\forall j,c,t) \qquad (19)$$

$$\sum_{e} Gt_{ejct} \leq NP_{jc} XP_{j} \qquad (\forall j,c,t) \qquad (20)$$

$$\text{Inv}_{ec1} = N_{ec} - \sum_{j} Gt_{ejc1} \qquad (\forall e,c) \qquad (21)$$

$$\text{Inv}_{ect} = \text{Inv}_{ec,t^{-}} - \sum_{j} Gt_{ejct} \qquad (\forall e,c,t>1) \qquad (22)$$

$$\sum_{c} Gt_{ejct} \leq \sum_{v} MPP_{v} UPPc_{vejt} \qquad (\forall e,j,t) \qquad (23)$$

$$\sum_{c} Gt_{ejct} \leq M_{e}^{E} Y_{je}\ (\forall e,j,t), Y_{je} \leq XP_{j} \qquad (\forall j,e) \qquad (24\text{-}25)$$

$$\sum_{e}\sum_{c} Gt_{ejct} \geq SL \cdot \left(\sum_{c} \text{DE}_{cjt}\right) XP_{j} \qquad (\forall j,t) \qquad (26)$$

$$\sum_{e}\sum_{j} UPPc_{vejt} \leq F_{v} \qquad (\forall v,t) \qquad (27)$$

$$\sum_{e}\sum_{j} \frac{OPP_{ej}}{\text{Speed}} UPPc_{vejt} \leq F_{v} \cdot \text{HrsMax} \qquad (\forall v,t) \qquad (28)$$

$$X_{i}, XP_{j}, Z_{di}, ZP_{dj}, Y_{je} \in \{0,1\}, U_{vdi}, UP_{vdj}, UPP_{vdh} \in \mathbb{Z}_{+}$$
$$L_{di}, LP_{dj}, LPP_{dh}, Gt_{ejct}, Wt_{cjt}, \text{Inv}_{ect}, UPPc_{vejt} \geq 0$$

Objective Function Initially, Equation (1) minimizes the overall objective function as a weighted sum of operational costs and shortage penalties; implying that the adjustment of weights determines the trade-off between economic savings and service level, thereby defining the decision-making orientation regarding cost versus shortage. Subsequently, Equation (2) meticulously aggregates cost components, including facility establishment costs, distance-

based transportation costs for all flows of people and goods, and components dependent on allocation decisions, to provide a realistic reflection of total system expenditures. Following this, Equation (3) aggregates shortages at the item, center, and time-period levels using priority weights, ensuring that the impact of imperfect service delivery on the ultimate goal is reflected in proportion to the criticality of different relief items.

Location and Allocation Constraints Regarding location and coverage, Equations (4) and (5) enforce the unique assignment of each affected area to exactly one temporary care center and one temporary shelter, ensuring a uniquely defined destination for the movement of outpatients and evacuees. On the other hand, Equations (6) and (7) restrict these assignments subject to coverage constraints; meaning an assignment is valid only if the distance falls within the permissible coverage radius of the facility; otherwise, it is effectively deactivated via a logical bound (Big-M). Furthermore, Equations (8) and (9) link each assignment to the operational status of the respective center, ensuring no area is connected to a closed facility, thereby preventing impractical routes. Finally, Equations (10) and (11) condition any flow of people on the activation of the corresponding assignment and control its magnitude via a large constant, preventing unwanted flows inconsistent with the allocation structure.

People Flow Constraints In the domain of human flows, Equation (12) mandates the complete evacuation of critically injured patients from every area to hospitals, establishing an input-output balance. Equations (13) and (14) then direct all outpatients and all evacuees to their designated destinations, ensuring no individual remains without a specified location. Subsequently, Equation (15) restricts the movement of outpatients on any route to the real seating capacity of the selected vehicles, preventing overloading beyond fleet capability. Additionally, Equation (16) caps the movement of evacuees by considering the effective capacity under uncertainty, ensuring decisions are adjusted conservatively against capacity fluctuations. Proceeding further, Equation (17) limits the transfer of critically injured patients to hospitals in proportion to the total capacity of deployed vehicles, preventing sudden congestion on specific routes. Finally, Equation (18) restricts the admission at each hospital using a capacity derived from a cautious approach towards uncertainty, ensuring patient distribution remains consistent with the real capability of medical centers.

Commodity Flow Constraints Regarding relief items, Equation (19) establishes the demand balance for each temporary shelter in every period; meaning the sum of shipments and recorded shortages must equal the demand of that period, leaving no demand unaccounted for. Simultaneously, Equation (20) limits the receiving/handling throughput of each shelter for every item per period according to its processing power, effectively preventing the flow of goods into closed centers. Conversely, Equation (21) determines the initial inventory of each distribution center at the start of the horizon based on initial stock minus first-period shipments, clarifying the process starting point. Equation (22) then carries this inventory over to the subsequent period, updating it by deducting shipments of the current period to guarantee temporal continuity and prevent shipping beyond available stock.

Transport Capacity and Service Level Concerning cargo transport capacity, Equation (23) aligns the volume of goods shipped on each route with the capacity procured through "continuous truck equivalents," establishing a balance between shipping demand and allocated vehicles. Moreover, Equation (24) conditions every cargo shipment on the activation of the respective route, effectively halting flow on inactive routes via a strict bound. Following this, Equation (25) links the activation of each route to the opening of the destination center,

ensuring no new route is activated towards a closed center, thereby maintaining logical network consistency. Finally, Equation (26) mandates a minimum periodic service level for active centers; implying that a certain percentage of demand in each period must be met, ensuring adherence to a minimum service standard throughout the time horizon.

Fleet Management Constraints At the fleet level, Equation (27) restricts the periodic utilization of truck equivalents for each vehicle type, ensuring coordination between available fleet capacity and the shipment schedule. Complementing this, Equation (28) controls the consumption of periodic driving hours based on distance and speed, ensuring that total travel times on routes do not exceed the permissible limit, thereby adhering to regulatory and safety considerations in fleet operation. Thus, compliance with operational fleet constraints and the achievement of the expected service level are simultaneously guaranteed.

Demand Forecasting

In the management of relief logistics, accurate demand forecasting is vital for determining optimal inventory levels and preventing shortages or overstocking, particularly during crises where demand is volatile and unpredictable. Under such conditions, demand forecasting based on historical data and predictive models provides an estimate of future requirements and enables the smooth continuity of operations. Due to the sporadic and stochastic nature of vital item consumption, the utilization of time-series models that extract past patterns, seasonal trends, and other data characteristics is a common method for estimating future demand and determining inventory levels and order quantities in subsequent periods.

In this study, ML techniques are employed to forecast the demand for relief items across various periods, with the aim of enhancing prediction accuracy compared to traditional methods. Time-series forecasting models, particularly those accounting for seasonal variations in demand, have been widely utilized in the context of relief item inventory management.

For instance, Kurawarwala and Matsuo (1998) investigated the effectiveness of demand forecasting regarding seasonal demand patterns using historical data and the Auto-Regressive Integrated Moving Average (ARIMA) model. This study demonstrated that the impact of seasonal variations on forecast accuracy is significant.

To improve forecast accuracy, Miller and Williams (2003) integrated seasonal factors derived from multiplicative models with their forecasting method. This approach is particularly beneficial in the context of relief item demand forecasting, where certain items experience higher demand during specific periods or under specific environmental conditions. This work was later extended by Miller and Williams (2003), who employed the Seasonal Auto-Regressive Integrated Moving Average (SARIMA) model—an extension of the ARIMA model—to model more complex relationships between trends and seasonality in time-series data. The SARIMA model has become one of the most prevalent methods for demand forecasting in relief item management, due to its ability to simultaneously account for seasonal effects and underlying trends)Ravuri & Vasundra, 2023(.

ARIMA Model

The ARIMA model is a method for fitting time series data to better understand or predict future points in the series (Fattah et al., 2018). The parameterization of ARIMA models involves three distinct integers (p, d, q). Consequently, ARIMA models are denoted as ARIMA(p, d, q). In datasets, these three parameters correspond to seasonality, trend, and noise.

- p represents the autoregressive component of the model. The effect of past values is incorporated by including them in the model.
- d represents the integrated component of the model. This parameter indicates the order of differencing (i.e., subtracting past time points from the current value) that needs to be applied to the time series.
- q corresponds to the moving average component of the model. Thus, the model error is calculated as a combination of previous errors at each past time point.

To address seasonal effects, Seasonal ARIMA is employed, which is denoted as ARIMA(p, d, q)(P, D, Q)_s. As previously mentioned, (p, d, q) are the non-seasonal parameters, whereas (P, D, Q) are analogous to (p, d, q) but are applied to the seasonal component of the time series.

- s represents the periodicity of the series (e.g., 4 for quarterly periods, 12 for annual periods, etc.).

Other Forecasting Models

In this section, alongside ARIMA and Seasonal ARIMA, brief descriptions of other forecasting models employed in this study are provided to enhance the comprehensibility of the research.

Simple Exponential Smoothing (SES)

SES is a simple and intuitive approach utilized in time-series forecasting. This method employs exponential smoothing to assign weights to past observations, thereby attributing greater importance to recent data. SES is particularly useful when no prominent trend or seasonal patterns exist within the data. Due to its ease of use and computational efficiency, it has become a popular choice for forecasting)Ostertagová & Ostertag, 2011(.

Long Short-Term Memory (LSTM)

LSTM is a variant of Recurrent Neural Networks (RNN) that has proven highly successful in capturing complex temporal dependencies. Unlike traditional feedforward neural networks, LSTM possesses a memory cell capable of storing information over long sequences. This characteristic makes LSTM suitable for modeling time-series data, including demand forecasting, where capturing both short-term and long-term dependencies is crucial)Hochreiter & Schmidhuber, 1997(.

By utilizing a combination of these diverse forecasting models, the objective was to comprehensively evaluate their performance in demand forecasting. The inclusion of ARIMA, SES, LSTM, and Seasonal ARIMA enabled the analysis of the strengths and weaknesses of each method.

The selected models—ARIMA, SES, LSTM, and Seasonal ARIMA—were chosen based on their proven effectiveness in time-series forecasting. ARIMA and Seasonal ARIMA are widely used for modeling trend and seasonality)ArunKumar et al., 2021(; SES is suitable for simple exponential smoothing)Hyndman & Athanasopoulos, 2018(; and LSTM is recognized for its ability to model complex temporal dependencies)Hochreiter & Schmidhuber, 1997(. By employing these diverse models, we aimed to comprehensively assess their performance and identify the most suitable model for demand forecasting.

To iteratively investigate various parameter combinations, Grid Search will be employed. The overall quality of each model for every parameter combination is evaluated, and the optimal set of parameters will be selected based on specific criteria. To assess and compare statistical models fitted with different parameters, and to rank them based on their ability to accurately predict future data points or how well they fit the data, the Akaike Information Criterion (AIC) value will be calculated. Models are evaluated based on their AIC, which measures the goodness of fit. Models that achieve the same level of fit with fewer features (parameters) will yield a lower AIC value compared to models with more features. Consequently, the model with the lowest AIC value will be selected.

Additionally, there are other metrics to calculate the error derived from the difference between actual and predicted values. To evaluate the accuracy of the models, the Mean Squared Error (MSE) is used, which is calculated as follows:

$$\textbf{Mean Squared Error (MSE)} = \frac{\sum_{i=1}^{N} e_i^2}{N} \quad (29)$$

In Equation 29:

- N represents the number of data points in the dataset.
- The term e_i denotes the forecast error for data point i, which is defined as the difference between the actual value and the predicted value for data point i.

$$e_i = \hat{y}_i - y_i \quad (30)$$

In Equation 30, $\hat{y}_i$ represents the predicted value, and y_i is the actual value.

Explanation:

MSE serves as a metric for evaluating the accuracy of forecasting models. This metric is derived by calculating the average of the squared differences between the actual and predicted values. A lower MSE value indicates higher model accuracy in forecasting. Due to the utilization of squared differences, MSE penalizes large errors; implying that models exhibiting larger deviations will yield higher MSE values. This metric is particularly beneficial in regression problems and time-series forecasting.

$$\textbf{Mean Absolute Percentage Error (MAPE)} = \frac{\sum_{i=1}^{N} \left| \frac{e_i}{y_i} \right|}{N} \quad (31)$$

Equation 31 indicates that the Mean Absolute Percentage Error (MAPE) is utilized to evaluate the accuracy of the models. MAPE constitutes another significant metric for assessing the accuracy of forecasting models. This metric represents the average of the absolute errors

expressed as a percentage of the actual values. A lower MAPE value corresponds to higher model accuracy.

Due to its reliance on percentages, MAPE facilitates the straightforward comparison of model performance across different scales. This metric is particularly advantageous in forecasting contexts where relative scales are of significance, such as demand forecasting.

4- Results

Machine Learning Model Results

This study utilizes the Python programming language, which is extensively employed in various domains, including machine learning and forecasting. As previously discussed, the Seasonal ARIMA model has been applied to forecast the demand for relief items. Monthly demand data for various items was collected from January 2021 to July 2025 to construct the dataset. This dataset was partitioned into training and testing sets. The training data comprises demand from January 2021 to March 2024, with the remaining data constituting the testing set. To evaluate the performance of different models with varying parameter sets, the AIC value was utilized.

For instance, the AIC, MSE, and MAPE values for different parameter sets in predicting the demand for Item 1 are presented in Table 3. According to this table, the lowest AIC value is 113.685, which was achieved by the ARIMA(0,1,1) × (0,1,1)12 set.

Based on Table 4, this study conducted a comparative analysis between the Seasonal ARIMA algorithm and three other popular time-series forecasting methods, namely ARIMA, SES, and LSTM. This comparison was executed using a Grid Search approach to determine the optimal parameter set for each algorithm. The results indicated that the Seasonal ARIMA model outperforms other techniques in terms of forecast error, as it achieved the lowest values for both MAPE and MSE metrics. Consequently, the findings suggest that the Seasonal ARIMA model is a superior forecasting method compared to the other techniques evaluated in this study. This implies that the Seasonal ARIMA model possesses a greater capability to identify hidden patterns and trends within the data and is capable of providing more accurate predictions of future demand patterns.

The superiority of the Seasonal ARIMA model over other algorithms can be attributed to its ability to model the seasonal, trend, and noise components of time-series data, rendering it a highly effective tool for forecasting item demand. Among the algorithms, the LSTM model yielded the poorest results. Several reasons may account for the underperformance of the LSTM model compared to the three other models (ARIMA, SARIMA, and SES). A primary reason is data insufficiency. LSTM models require a large volume of data to learn the complex patterns and relationships present within the data. If the dataset is relatively small, the LSTM model may fail to learn meaningful patterns and consequently exhibit inferior performance compared to simpler models such as ARIMA and SES.

Table 3. Performance results of demand forecasting for Item 1

(p,d,q)	(P,D,Q)s	AIC	MSE	MAPE

(0, 1, 1)	(0, 1, 1, 12)	113.685521	105.078	0.03613
(1, 1, 1)	(0, 1, 1, 12)	113.864314	94.0515	0.0344
(1, 1, 1)	(1, 1, 1, 12)	114.252153	99.9752	0.03447
(0, 1, 1)	(1, 1, 1, 12)	114.877974	103.254	0.03477
(1, 0, 1)	(0, 1, 1, 12)	120.773696	99.3739	0.03511
...	...	...	...	...
(1, 1, 0)	(0, 0, 1, 12)	1365.13544	3455.14	0.23403
(1, 0, 0)	(0, 0, 1, 12)	1486.33075	4049.17	0.25423
(0, 0, 1)	(1, 0, 1, 12)	2062.64128	893.351	0.1086
(0, 0, 1)	(0, 0, 1, 12)	2185.31442	63096.1	1

Table 4. MSE and MAPE values of the optimal forecasting algorithms

Model	MSE	MAPE
ARIMA	3462.82	23.43%
SES	3455.08	23.40%
SARIMA	105.08	3.61%
LSTM	1521.69	12.83%

Case Study

This case study addresses a post-earthquake urban scenario comprising two affected areas, two temporary care centers, two temporary shelters, two hospitals, and two distribution centers. The planning horizon spans 48 hours, discretized into six 8-hour periods. Three population groups—"outpatients," "evacuees" (those requiring shelter), and "critically injured"—are directed to temporary care centers, temporary shelters, and hospitals, respectively. The flow of relief items is sourced from distribution centers and dispatched to temporary shelters. Decisions regarding facility opening/closing, area allocation, and the transportation schedule for people and goods are optimized simultaneously within a MILP framework.

Throughout the horizon, a minimum of 80% of the demand in each period for every temporary shelter must be satisfied, while the remaining 20% is permissible as controlled shortage. Uncertainty regarding hospital admission capacities and the passenger capacity of vehicles transporting evacuees is modeled using triangular fuzzy numbers and converted into linear crisp equivalents via a confidence parameter of 0.8 to maintain exact and efficient solvability.

Data and Settings

The numerical analysis simulates a post-earthquake response scenario over a 48-hour planning horizon, divided into six 8-hour operational periods. The network topology explicitly consists of 2 affected areas (demand origins), 2 candidate temporary care centers, 2 candidate temporary shelters, 2 hospitals, and 2 distribution centers.

Effective distances between areas, centers, and hospitals have been extracted from the operational map and standardized into distance units. Key operational parameters, detailed in Table 5, were selected to reflect realistic constraints:

- Transportation Costs: Vehicle operating costs are set at 5 and 8 monetary units per distance unit for Type 2 and Type 1 vehicles, respectively.
- Capacities: Cargo fleet capacities are defined at 1,700 and 2,000 units per truck-equivalent55. To model uncertainty, hospital admission capacities are represented as triangular fuzzy numbers, (100, 110, 120) and (150, 160, 170).
- Demand: Relief item demand is dynamic, covering 6 types of relief items, with total forecasted demand for specific shelters reaching up to 480 units per period for high-priority goods.

The periodic handling capacity for each item at every temporary shelter is defined, and the initial inventory of each item is injected into distribution centers at the beginning of the horizon. For the cargo fleet, a "continuous truck equivalent" variable is employed to facilitate flexible and linear capacity allocation; constraints regarding fleet size and driving hours are also enforced for each period. Finally, a weighted objective function, with a cost weight of 1 and a shortage weight of 3.5, establishes the trade-off between cost and service level. This configuration allows for the evaluation of the model's performance under tight capacity constraints and varying service level requirements.

Table 5. Selected parameters of the case study

Category	Parameter	Value / Vector
Horizon & Service	Number of periods	6 (8-hour periods)
	Minimum Service Level	0.80
Objectives	Cost Weight	1.0
	Shortage Weight	3.5
Fuzzy Logic	Confidence Parameter	0.80
Vehicle (Cost)	Cost per unit distance (Type 1)	8
	Cost per unit distance (Type 2)	5
Vehicle (Passenger)	Passenger Capacity (Type 1)	3
	Passenger Capacity (Type 2)	4
Vehicle (Fuzzy Pax)	Triangular Capacity (Type 1)	(4, 5, 6)
	Triangular Capacity (Type 2)	(5, 6, 7)
Vehicle (Cargo)	Cargo Capacity (Type 1)	2000
	Cargo Capacity (Type 2)	1700
Cargo Fleet	Available Quantity (Type 1)	0
	Available Quantity (Type 2)	2
Road Operations	Max Hours per Vehicle per Period	8
	Average Speed	60
Total 48h Demand	**Temp Shelter 1** (6 items)	[310, 350, 320, 200, 260, 180]
	Temp Shelter 2 (6 items)	[360, 370, 380, 240, 280, 220]

Periodic Capacity	**Temp Shelter 1** (6 items)	[350, 380, 400, 300, 320, 280]
	Temp Shelter 2 (6 items)	[420, 450, 480, 350, 360, 340]
Initial Inventory	**Distribution Center 1** (6 items)	[1000, 1200, 1400, 900, 1100, 800]
	Distribution Center 2 (6 items)	[1500, 1400, 1300, 1000, 900, 950]
Fuzzy Hospital Cap.	**Hospital 1** (Triangular)	(100, 110, 120)
	Hospital 2 (Triangular)	(150, 160, 170)

Solution Configuration and Metrics

The problem is formulated as a MILP model and solved using a standard solver. The evaluation of solution quality is conducted based on three metrics: the value of the weighted objective function, adherence to the periodic service level in temporary shelters, and the consumption of transport resources (truck equivalents and driving hours) relative to permissible caps. In addition to the baseline scenario, a sensitivity analysis on the shortage weight and the fuzzy confidence parameter is proposed to examine the trade-offs between cost and service, as well as conservative policies.

Case Study Results and Interpretation

The model results (obtained using GAMS and the BARON solver) indicate that in the optimal solution, one temporary care center (Center 1) and both temporary shelters (Centers 1 and 2) are established. Both affected areas are assigned to Care Center 1; regarding shelter allocation, Area 1 is assigned to Shelter 2, and Area 2 is assigned to Shelter 1. This configuration is consistent with concentrating commodity flows on the two lower-cost routes from distribution centers to shelters. All outpatients and critically injured patients have been allocated to their respective centers and hospitals according to the population of each area, and coverage and capacity constraints have not been violated.

The 80% service level constraint is active in all periods; the remaining 20% is recorded as controlled shortage, primarily concentrated on Item 5 (and partially Item 2), as their shortage penalties are lower than transportation costs. Consequently, the shortage stems from an economic decision rather than an inventory stockout. The cargo fleet utilizes only Vehicle Type 2 on two main routes with low utilization intensity, and constraints on vehicle count and driving hours remain non-binding, indicating the existence of a capacity buffer for more severe scenarios.

In the event of increasing the shortage weight or the minimum service level (e.g., from 80% to 90%), shortage decreases while transportation costs rise; conversely, reducing the shortage weight lowers costs but increases shortage. Tables 6 and 7 provide a summary of the case study solution results.

Table 6. Summary of Case Study Solution Results

Component	Value / Interpretation
Objective Function Components	Z_1 = 649,294.559; Z_2 = 239.000; OBJ = 650,131.059
Facility Status	**Temp Care Center:** Only Index 1 Open**, Temp Shelters:** Indices 1 & 2 Open
Allocation to Temp Care	Both areas assigned to **Temp Care Center 1**
Allocation to Temp Shelters	**Area 1** assigned to Shelter 2, **Area 2** assigned to Shelter 1
Periodic Service Level	≅80 % for both Temp Shelters (**Active bound**)
Cargo Fleet Usage	**Vehicle Type 2** on two main routes; approx. 0.127 and 0.145 equivalents per period
Shortage Pattern	Concentrated on **Item 5** and partially **Item 2**; higher priority items fully supplied

Table 7. Shortage of commodities

Item / Commodity	Total Demand	Total Shipment	Total Shortage	Shortage Share(%)	Contribution to Z2
1	670	670	0	0٪	0
2	720	566	154	21.4٪	77.0
3	700	700	0	0٪	0
4	440	440	0	0٪	0
5	540	0	540	100٪	162.0
6	400	400	0	0٪	0
Total	**3,470**	**2,776**	**694**	**20.0٪**	**239.0**

Sensitivity Analysis

Effect of Service Level

To investigate the impact of variations in service level on model performance, a sensitivity analysis was conducted using different values of $SL \in \{0.7, 0.8, 0.85, 0.90, 0.95\}$. The obtained results indicate that variations in service level exert distinct effects on operational costs, shortages, fleet utilization intensity, and commodity supply patterns.

Impact on Costs: As observed in Figure 2, increasing the service level leads to a substantial reduction in shortages while simultaneously causing a moderate increase in operational costs. For instance, as the service level rises from 0.70 to 0.95, shortage costs have decreased by over 80%, whereas the total cost has increased by only approximately 3,000 units. This demonstrates the existence of a fundamental trade-off: at lower levels, increasing the service level results in a major reduction in shortages at a limited cost; however, at higher levels, reducing shortages is achievable only through a significant increase in costs. Therefore, the cost-shortage relationship is non-linear, and diminishing returns are observed as higher service levels are approached.

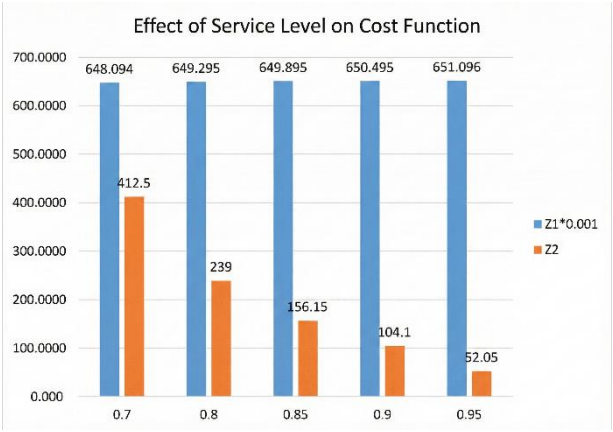

Figure 2. Effect of service level on cost function

Impact on Fleet Usage on Main Routes: The results indicate that, as depicted in Figure 3, the intensity of fleet utilization on main routes increases in an approximately linear manner as the service level rises. Specifically, the route from Distribution Center 1 to Temporary Shelter 2 and the route from Distribution Center 2 to Temporary Shelter 1 contribute the most to this growth. At lower levels, an increase in service level results in a more rapid surge in fleet consumption, as the model prioritizes addressing "cheaper" shortages first. However, from the 0.85 level upwards, the growth in fleet consumption proceeds at a steadier pace, indicating that satisfying the remaining shortages necessitates the allocation of resources to higher-cost items.

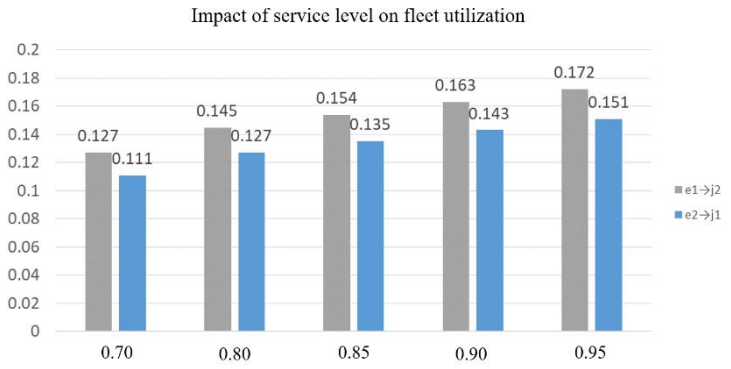

Figure 3. Impact of service level on fleet utilization

Shortage Pattern of Items: Figure 4 illustrates how the pattern of shortages changes at the item level. At low service levels, shortages occur in both medium-priority items and high-cost items. However, from a service level of 0.85 upward, shortages in medium-priority items are completely eliminated, and the remaining shortages shift toward higher-cost, harder-to-supply items. For example, at the 0.85 level, Item 2 no longer experiences any shortages, whereas Item 5 still faces shortages that only gradually decrease as the service level increases. This trend clearly reflects the logic of the model: it first addresses the lower-cost shortages and then, in subsequent stages, reduces the higher-cost shortages.

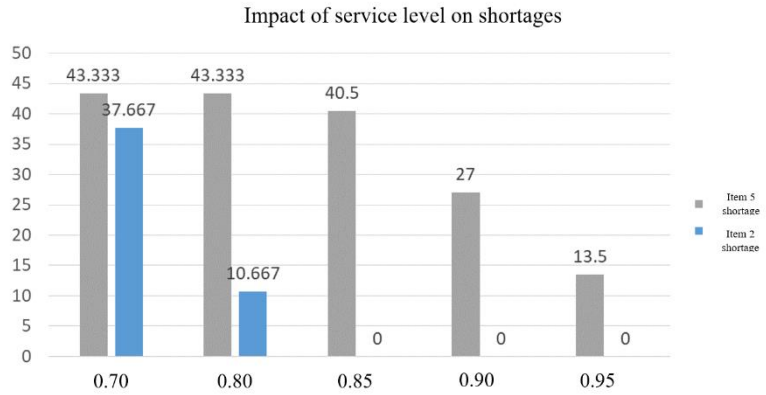

Figure 4. Impact of service level on fleet utilization

Managerial Insights

- There is a nonlinear trade-off between operational cost and service level: initial increases in service level sharply reduce shortages while adding relatively little cost, but at higher levels, each additional unit of improvement imposes a substantial cost. A service level of around 0.85 can be considered a reasonable balance point between cost and humanitarian responsiveness.
- As the service level increases, shortages gradually become concentrated in items that are logistically expensive to supply; therefore, addressing these remaining shortages requires strategies such as pre-positioning, local procurement, and targeted support.
- Utilization of the transportation fleet grows almost linearly with increasing service level and is mainly concentrated on low-cost routes; this pattern allows managers to better predict additional needs in driving hours, number of vehicles, and fuel, and to scale operations more reliably.
- Pursuing very high service levels (e.g., above 0.9) has limited practical value because the remaining shortage reduction occurs primarily in very high-cost items and leads to a steep surge in total cost; therefore, it is recommended to strike a balance between maximizing coverage and maintaining financial sustainability.

Effect of W_2/W_1

Based on the sensitivity analysis, the ratio of the shortage penalty weight (W2) to the cost weight (W1) fundamentally governs the model's strategic and operational decisions. Increasing this ratio creates a clear and logical transition from a cost-oriented logistics model to a service-level-oriented logistics model, as detailed in the analysis below.

Effect on Costs: As shown in Figure 5, the relationship between total operational cost (Z1) and weighted unmet demand (Z2) follows a well-defined Pareto frontier, reflecting the inherent economic trade-off in the system. At low penalty ratios ($W2/W1 \in \{1,2\}$), the optimization prioritizes economic efficiency, resulting in a solution with minimum cost (Z1=6,464,146) at the expense of significant service failure, with a weighted shortage of (Z2=1362). In this case,

the financial penalty for unmet demand is insufficient to justify investment in network expansion or increased transportation capacity.

A strategic turning point occurs at the ratio W2/W1=3.5. At this threshold, the shortage penalty becomes high enough to necessitate a fundamental reconfiguration of the relief network. The model decides to reopen the second shelter center, a decision that increases total cost by about 0.5%, raising it to Z1=6,492,94. This investment in network infrastructure enables a substantial improvement in service level, reducing the weighted shortage (Z2) by more than 82% to 239. Beyond this point, the system exhibits diminishing returns. Increasing the penalty further to W2/W1=7 results in only a slight rise in cost to Z1=6,495,11, which in turn yields only a modest reduction in shortage to Z2=207. This indicates a shift from large-scale strategic investments toward more fine-tuned and costlier operational adjustments.

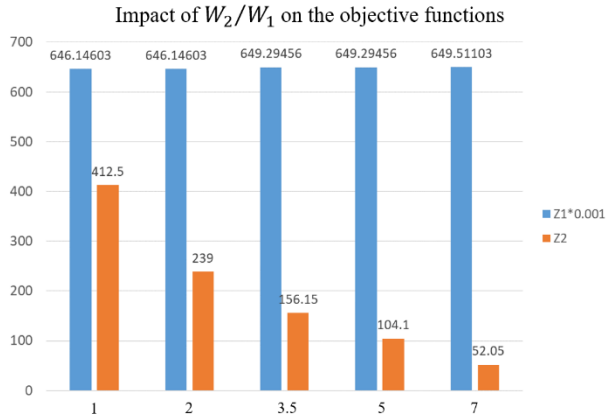

Figure 5. Effect of the Objective Function Weight Ratio on the Total Cost Function

Effect on Fleet Utilization: Figure 6 illustrates how the strategic decisions observed on the Pareto frontier are directly reflected in the configuration of the logistics network and the intensity of fleet operations. The solution for low penalty weights W2/W1∈{1,2} corresponds to a lean operational state in which only one shelter center is active. This minimal network is served by a baseline fleet deployment equivalent to 0.762 full truck trips for vehicle type 2 over the planning horizon.

The strategic shift at W2/W1=3.5 leads to a substantial intensification of logistics activities. Reopening the second shelter center activates new transportation routes between distribution centers and demand points. As a result, the required fleet capacity more than doubles, with the total equivalent truck trips increasing to 1.632. This significant increase in vehicle deployment serves as the primary operational mechanism for reducing unmet demand and directly justifies the corresponding rise in total cost Z1.

With a further increase in the penalty ratio to 7, a final but modest intensification occurs, as fleet utilization reaches 1.668 equivalent truck trips, indicating the additional effort needed to serve the last remaining segments of high-priority demand.

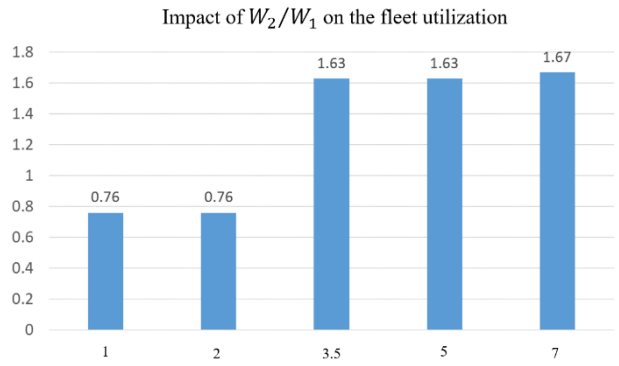

Figure 6. Effect of the Objective Function Weight Ratio on the fleet utilization

Effect on Item Shortages: The priority-based approach to resource allocation is detailed in Figure 7, which shows how the model satisfies demand according to predefined item-importance weights. In the initial cost-oriented solutions W2/W1∈{1,2}, shortages are widespread and affect all logistics categories, including those with the highest priority rankings.

Following the network expansion at W2/W1=3, the additional logistics capacity is not deployed indiscriminately. Instead, it is precisely directed toward eliminating unmet demand for more critical items. The results show that shortages for items 1, 3, 4, and 6—each of which carries a high priority value—are fully eliminated. In contrast, shortages persist for lower-priority items such as item 2, because the model assesses the cost of supplying them as higher than their weighted penalty.

When the penalty ratio increases to 7, the model proceeds to the next priority tier and allocates additional resources to eliminate the remaining shortage of item 2 at Shelter 1. This hierarchical approach ensures that the most critical needs are met first, thereby maximizing humanitarian impact for any given budget level.

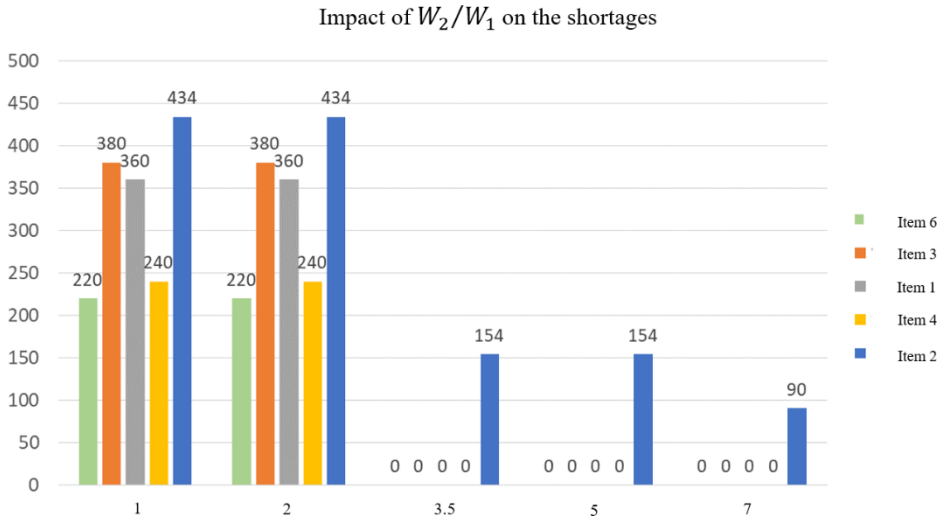

Figure 7. Effect of the Objective Function Weight Ratio on the shortages

Managerial Insights

- **Optimal Financing:** The cost–service-level relationship is convex and nonlinear; there exists an "optimal" budget threshold at which small increases in resources yield the greatest improvement in humanitarian outcomes. The model should be used to identify and justify this financing threshold, rather than merely executing a fixed budget.
- **Input-Driven Structural Breakpoints:** The strategic shift from a single-shelter to a two-shelter network at the threshold W2/W1=3.5 is directly triggered by the interaction between SARIMA-forecasted demand peaks and fuzzy capacity constraints. Specifically, the ML module predicted distinct demand surges in periods 3 and 4 that exceeded the conservative fuzzy capacity limits of a single facility (calculated at β=0.8). At lower penalty ratios, the model found it economical to accept shortages during these peaks; however, at W2/W1=3.5, the weighted penalty for this specific volume of unmet demand surpassed the establishment cost of Shelter 2. This highlights that network design decisions are not static but are highly sensitive to the accuracy of peak-demand detection provided by the forecasting module.
- **Network design matters more than micro-optimizing operations:** The largest reduction in shortages (e.g., by opening a second shelter center) comes from structural network decisions rather than fine-tuning routes and schedules. Therefore, in pre-crisis planning, network design and the pre-qualification of shelter and distribution center locations should be prioritized.
- **A formal item-priority system:** Under shortage conditions, the model systematically prioritizes the supply of critical items—provided that a quantitative priority hierarchy is defined. Organizations should embed such a priority system in their inventory and logistics platforms so that water, medicine, and life-saving supplies always receive top allocation.
- **Optimization as a strategic simulator:** The model's main value is not in producing a fixed plan, but in enabling the exploration of scenarios, trade-offs, and stress-testing resilience against shocks such as budget cuts or demand surges. Continuous use of the model can strengthen agile, data-driven decision-making within the organization.

5- Conclusion

This study presented an integrated framework for designing a post-earthquake humanitarian supply chain network in which facility location–allocation, fleet planning, and simultaneous flows of people and relief items were combined within a mixed-integer linear programming model, supported by machine-learning-based demand forecasting and fuzzy modeling of capacity uncertainty. The weighted objective function clarified the cost/service-level trade-off and enabled policy tuning.

The results showed that combining data-driven forecasting with a conservative treatment of uncertainty reduces item shortages and response time, and achieves higher population coverage with fewer but more optimally located facilities. The key managerial insights include: (1) the necessity of a dynamic forecasting module for critical items; (2) establishing periodic service-level floors to guarantee minimum supply at every active center; (3) joint allocation of the fleet

for transporting both people and goods rather than using separate policies; and (4) using effective fuzzy capacities to avoid overly optimistic planning.

However, the study has limitations: the network scale and number of items/periods are constrained; travel times and congestion are simplified; and decision coordination is assumed to be centralized. Additionally, the accuracy of the forecasting module depends on the quality of historical data.

Future research directions include: hybrid deep learning with exogenous variables, online updating with streaming data, distributionally robust optimization, modeling congestion and network disruption, incorporating spatial–social fairness constraints, linking with agent-based evacuation models, and developing real-time decision-support systems. This framework can serve as a practical foundation for designing resilient humanitarian networks in other crisis scenarios.

References

Ahamed, B. S., Poornima, D., Sheela, A. S., & Nivetha, S. (2023). Allocation of Resources in the Cloud Conducted Efficiently Through the Use of Machine Learning. 2023 International Conference on Emerging Research in Computational Science (ICERCS),

Ahmad, M., Tayyab, M., & Habib, M. S. (2025). An enhanced deep reinforcement learning approach for efficient, effective, and equitable disaster relief distribution. *Engineering Applications of Artificial Intelligence*, *143*, 110002.

Aliahmadi, A., Jafari-Eskandari, M., Mozafari, M., & Nozari, H. (2013). Comparing artificial neural networks and regression methods for predicting crude oil exports. International Journal of Information, Business and Management, 5(2), 40-58.

ArunKumar, K., Kalaga, D. V., Kumar, C. M. S., Chilkoor, G., Kawaji, M., & Brenza, T. M. (2021). Forecasting the dynamics of cumulative COVID-19 cases (confirmed, recovered and deaths) for top-16 countries using statistical machine learning models: Auto-Regressive Integrated Moving Average (ARIMA) and Seasonal Auto-Regressive Integrated Moving Average (SARIMA). *Applied soft computing*, *103*, 107161.

Bahmani, H., Ao, Y., Li, M., Yang, D., & Wang, D. (2023). Dual disasters: Seismic evacuation decision-making during COVID-19 lockdown: A case study of Luding earthquake, Sichuan Province. *Journal of transport geography*, *110*, 103622.

Bakhshian, E., & Martinez-Pastor, B. (2023). Evaluating human behaviour during a disaster evacuation process: A literature review. *Journal of traffic and transportation engineering (English edition)*, *10*(4), 485-507.

Basu, S., Roy, S., Bandyopadhyay, S., & Bit, S. D. (2018). A utility driven post disaster emergency resource allocation system using DTN. *IEEE Transactions on Systems, Man, and Cybernetics: Systems*, *50*(7), 2338-2350.

Batur, M., Alkan, R. M., Karaman, H., & Özener, H. (2025). Multi-dimensional optimization of nuclear emergency shelters: balancing capacity, evacuation efficiency, and supply accessibility. *International Journal of Engineering and Geosciences*, *10*(2), 244-261.

Baygan, B., Mehrabian, A., Yousefi Nejad Attari, M., & Doostideilami, M. J. (2024). A Bi-Objective Stochastic Model of Locating-Allocating-Routing Relief and Rescue in Disaster Response Conditions: An Accelerated Benders Decomposition. *Complexity*, *2024*(1), 8838354.

Bier, M., Fathi, R., Stephan, C., Kahl, A., Fiedrich, F., & Fekete, A. (2025). Spontaneous volunteers and the flood disaster 2021 in Germany: Development of social innovations in flood risk management. *Journal of Flood Risk Management*, *18*(1), e12933.

Chobar, A. P., Adibi, M. A., & Kazemi, A. (2025). Multi-objective hub-spoke network design of perishable tourism products using combination machine learning and meta-heuristic algorithms. *Environment, development and sustainability*, *27*(10), 23237-23264.

Du, S., Town, H., & District, P. (2024). Evacuation route planning in disaster situations. Proc. of SPIE Vol,

Emami, A., Hazrati, R., Delshad, M. M., Pouri, K., Khasraghi, A. S., & Chobar, A. P. (2024). A novel mathematical model for emergency transfer point and facility location. *Journal of Engineering Research*, *12*(1), 182-191.

Fattah, J., Ezzine, L., Aman, Z., El Moussami, H., & Lachhab, A. (2018). Forecasting of demand using ARIMA model. *International Journal of Engineering Business Management*, *10*, 1847979018808673.

Geng, S., Gong, Y., Hou, H., Yang, J., & Onggo, B. S. (2024). Resource management in disaster relief: a bibliometric and content-analysis-based literature review. *Annals of Operations Research*, *343*(1), 263-292.

Ghasemi, F., Khadem, M., & Chobar, A. P. (2023). Supplier Selection for Supply Chain by Risk-Averse Decision Maker with Multi-Criteria Decision Making. *International journal of industrial engineering and operational research*, *5*(3), 50-62.

Ghasemi, P., Goodarzian, F., & Abraham, A. (2022). A new humanitarian relief logistic network for multi-objective optimization under stochastic programming. *Applied Intelligence (Dordrecht, Netherlands)*, *52*(12), 13729.

Hochreiter, S., & Schmidhuber, J. (1997). Long short-term memory. *Neural computation*, *9*(8), 1735-1780.

Hyndman, R. J., & Athanasopoulos, G. (2018). *Forecasting: principles and practice*. OTexts.

Iraj, M., Chobar, A. P., Peivandizadeh, A., & Abolghasemian, M. (2024). Presenting a two-echelon multi-objective supply chain model considering the expiration date of products and solving it by applying MODM. *Sustainable Manufacturing and Service Economics*, 3, 100022.

Jabal-Ameli, M. S., Bozorgi-Amiri, A., & Heydari, M. (2011). A multi-objective possibilistic programming model for relief logistics problem.

Jha, A., Acharya, D., & Tiwari, M. (2017). Humanitarian relief supply chain: a multi-objective model and solution. *Sādhanā*, *42*(7), 1167-1174.

Kurawarwala, A. A., & Matsuo, H. (1998). Product growth models for medium-term forecasting of short life cycle products. *Technological Forecasting and Social Change*, *57*(3), 169-196.

Long, Y., Sun, P., & Xu, G. (2024). Dynamic heterogeneous resource allocation in post-disaster relief operation considering fairness. *Advanced Engineering Informatics*, *62*, 102858.

Lu, M. (2024). Application of machine learning algorithms in resource allocation for wireless communications. *Applied and Computational Engineering*, *102*, 37-42.

Ma, Y.-W., & Chiang, Y.-N. (2024). A Postdisaster Network Resource Allocation in a Mobile Communication Network. *IT Professional*, *26*(4), 48-54.

Mao, Q., & Ma, H. (2025). Optimization of Emergency Shelter Siting and Material Distribution Considering Multiple Psychological Perceptions of Disaster Victims Under Two-Dimensional Fairness Measurement. *Transportation Research Record*, 03611981251315686.

Miller, D. M., & Williams, D. (2003). Shrinkage estimators of time series seasonal factors and their effect on forecasting accuracy. *International Journal of Forecasting*, *19*(4), 669-684.

Movahed, A. B., Movahed, A. B., & Nozari, H. (2024). Opportunities and challenges of smart supply chain in Industry 5.0. Information Logistics for Organizational Empowerment and Effective Supply Chain Management, 108-138.

Naderipour, M., & Salandari Rabari, M. M. (2024). *Applying deep learning methods for blood supply chain demand prediction (Case study: Afzalipour Hospital in Kerman)* 10th International Conference on Industrial Engineering and Systems, https://civilica.com/doc/2119516

Nozari, H., Tavakkoli-Moghaddam, R., Rohaninejad, M., & Hanzalek, Z. (2023, September). Artificial intelligence of things (AIoT) strategies for a smart sustainable-resilient supply chain. In IFIP

International Conference on Advances in Production Management Systems (pp. 805-816). Cham: Springer Nature Switzerland.

Ostertagová, E., & Ostertag, O. (2011). The simple exponential smoothing model. The 4th International Conference on modelling of mechanical and mechatronic systems, Technical University of Košice, Slovak Republic, Proceedings of Conference,

Pal, B., Paul, S., Turuk, A. K., Rahaman, M. M., & Patel, S. (2024). UAV Aided Post Disaster Relief Networks using Blockchain Technology: Challenges and Solutions. 2024 Eighth International Conference on Parallel, Distributed and Grid Computing (PDGC),

Rahmawaty, M. A., & Hasan, A. F. (2023). Mapping The Location of Flood Shelters in Demak Regency using The Spatial Multi Criteria Evaluation Method. IOP Conference Series: Earth and Environmental Science,

Raj, V. H., Sreevani, N., Thethi, H. P., Nainwal, A., Ziara, S., & Kumari, M. S. (2024). Blockchain and Machine Learning for Predictive Resource Distribution in Disaster Response Management. 2024 1st International Conference on Sustainable Computing and Integrated Communication in Changing Landscape of AI (ICSCAI),

Ravuri, V., & Vasundra, D. S. (2023). An effective weather forecasting method using a deep long–short-term memory network based on time-series data with sparse fuzzy c-means clustering. *Engineering Optimization*, *55*(9), 1437-1455.

Saeedi, A., & Dejpasand, M. (2024). Investigation and analysis of temporary shelter site selection in crisis conditions with emphasis on man-made threats (Case study: District 1 of Kermanshah). *Passive Defense*, *15*(4), 11-24.

Saeidian, B., Mesgari, M. S., Pradhan, B., & Ghodousi, M. (2018). Optimized location-allocation of earthquake relief centers using PSO and ACO, complemented by GIS, clustering, and TOPSIS. *ISPRS international journal of geo-information*, *7*(8), 292.

Salazar, A. T., Medrano, M., Medina, M. D., Roa, J., & Pesantez, J. E. (2024). Enhancing Evacuation Warning Responsiveness: Exploring the Impact of Social Interactions through an Agent-Based Model Approach.

Setiawan, E., Liu, J., & French, A. (2019). Resource location for relief distribution and victim evacuation after a sudden-onset disaster. *IISE transactions*, *51*(8), 830-846.

Smyrnakis, M., & Galla, T. (2014). Decentralized optimisation of resource allocation in disaster management. In *City Evacuations: An Interdisciplinary Approach* (pp. 89-106). Springer.

Tang, K., & Osaragi, T. (2024). Multi-objective distributionally robust optimization for earthquake shelter planning under demand uncertainties. *GeoHazards*, *5*(4), 1308-1325.

Tang, L., Zhou, J., Zhou, L., & Xing, H. (2025). Exploring the effects of perception factors on evacuation intentions of residents. *Journal of Mountain Science*, *22*(2), 592-610.

Veisi, O., Heydari, J., Razmi, J., & Sangari, M. S. (2019). Optimization of distribution and support pattern in the supply chain of logistics and support system under dynamic and uncertain conditions. *Quarterly Journal of Military Management*, *19*(74), 81-116. https://jmm.iranjournals.ir/article_38054_be61a669772d4f02117fa9c9ddc2a11a.pdf

Wagner, S. M., Ramkumar, M., Kumar, G., & Schoenherr, T. (2024). Supporting disaster relief operations through RFID: enabling visibility and coordination. *The International Journal of Logistics Management*, *35*(6), 1681-1712.

Wang, J., Shen, D., & Yu, M. (2020). Multiobjective optimization on hierarchical refugee evacuation and resource allocation for disaster management. *Mathematical Problems in Engineering*, *2020*(1), 8395714.

Woo, S. J., & Kang, S. (2025). Optimising Shelter Locations for Bus Evacuation and Relief Supply Under Traffic Congestion. *IET Intelligent Transport Systems*, *19*(1), e70020.

Xie, H., Zhan, Y., & Fang, X. (2024). Resource allocation for satellite communication network of emergency communications in distribution network. 2024 International Wireless Communications and Mobile Computing (IWCMC),

Yang, Z., Martí, A., Chen, Y., & Martí, J. R. (2022). Optimal resource allocation to enhance power grid resilience against hurricanes. *IEEE Transactions on Power Systems*, *38*(3), 2621-2629.

Yazdani, M., & Haghani, M. (2023). Elderly people evacuation planning in response to extreme flood events using optimisation-based decision-making systems: A case study in western Sydney,

Australia. *Knowledge-Based Systems*, *274*, 110629. https://doi.org/https://doi.org/10.1016/j.knosys.2023.110629

Yu, L., Zhang, C., Jiang, J., Yang, H., & Shang, H. (2021). Reinforcement learning approach for resource allocation in humanitarian logistics. *Expert Systems with Applications*, *173*, 114663.

Yuichi Koido, M. (2023). Current Status of the Disaster Health, Medical, and Welfare Coordination in Japan. *Prehosp. Disaster Med*, *38*(S1), s123-s124.

Zhang, H., Zhao, X., Fang, X., & Chen, B. (2024). Proactive resource request for disaster response: A deep learning-based optimization model. *Information Systems Research*, *35*(2), 528-550.